

# Composite Hybrid Cluster Built from the Integration of Polyoxometalate and a Metal Halide Cluster: Synthetic Strategy, Structure, and Properties

Xin-Xiong Li,<sup>†</sup> Xiang Ma,<sup>†</sup> Wen-Xu Zheng,<sup>†</sup> Yan-Jie Qi,<sup>†</sup> Shou-Tian Zheng,<sup>\*,†</sup> and Guo-Yu Yang<sup>\*,‡</sup>

<sup>†</sup>State Key Laboratory of Photocatalysis on Energy and Environment, College of Chemistry, Fuzhou University, Fuzhou, Fujian 350108, China

<sup>‡</sup>MOE Key Laboratory of Cluster Science, School of Chemistry, Beijing Institute of Technology, Beijing 100081, China

## Supporting Information

**ABSTRACT:** A step-by-step synthetic strategy, setting up a bridge between the polyoxometalate (POM) and metal halide cluster (MHC) systems, is demonstrated to construct an unprecedented composite hybrid cluster built up from one high-nuclearity cationic MHC  $[\text{Cu}_8\text{I}_6]^{2+}$  and eight Anderson-type anionic POMs  $[\text{HCrMo}_6\text{O}_{18}(\text{OH})_6]^{2-}$  cross-linked by a tripodal alcohol derivative.

The construction of crystalline materials with composite structures through integration of entirely different components [e.g., the introduction of polyoxometalates (POMs) into metal–organic frameworks] is of great interest because such materials usually have novel structures and various properties derived from different components.<sup>1,2</sup> Of particular importance is the development of such composite materials to study the crossover field of different research systems.

POMs are a class of metal–oxo clusters with metals in high oxidation states (metals here generally refer to vanadium, molybdenum, tungsten, niobium, and tantalum). Owing to the unique structural features, acid–base and electrical properties, POMs exhibit a wide range of applications in multiple areas such as catalysis, magnetism, and materials science.<sup>3</sup> Compared with POMs, metal halide clusters (MHCs) are kinds of completely different metal clusters that are usually built from low-valence metals (e.g.,  $\text{Cu}^+$ ,  $\text{Ag}^+$ ,  $\text{Pb}^{2+}$ , and so on) hold together by halide ions, such as a  $\text{Cu}_4\text{I}_4$  cubane tetramer and a  $\text{Cu}_6\text{I}_6$  hexagonal prism.<sup>4</sup> MHCs are currently attracting great attention for their diverse structural topologies and potential applications in catalysis, biology, and luminescent materials.<sup>5</sup>

Considering the remarkably different structural features between POMs and MHCs and their respective intriguing properties, the development of brand new composite structures incorporating both POMs and MHCs is of great interest. However, because of the lack of feasible synthetic strategies, the integration of MHCs into POMs remains largely unexplored. Especially, the construction of inorganic–organic hybrid POM–MHC-based composite structures is a challenge for synthetic chemists. This is because POMs are oxygen-rich polyoxoanions, which are not easy to directly coordinate with organic ligands (e.g., common carboxylate or nitrogen-containing ligands) under conventional solution or hydrothermal conditions. In contrast,

MHCs usually have unsaturated metal sites and replaceable terminal halides, which often act as secondary building blocks to coordinate with organic ligands via metal–oxygen/nitrogen bonds to form extended hybrid frameworks. So, to explore specific organic ligands with the ability of bridging both POMs and MHCs might pave the way for creating fascinating inorganic–organic hybrid POM–MHC-based composite materials.

Herein, we report the first inorganic–organic hybrid POM–MHC-based composite cluster  $(\text{TBA})_{14}[\text{Cu}_8\text{I}_6][\text{HCrMo}_6\text{O}_{18}(-\text{OH})_3\text{L}]_8$  [**1**; TBA =  $n\text{Bu}_4\text{N}^+$  and L = 2-(hydroxymethyl)-2-(pyridin-4-yl)-1,3-propanediol] built from cuprous iodide cluster  $[\text{Cu}_8\text{I}_6]^{2+}$  and Anderson-type polyoxomolybdates  $[\text{HCrMo}_6\text{O}_{18}(\text{OH})_6]^{2-}$  joined together by a tripodal alcohol derivative, demonstrating a general step-by-step synthetic strategy for making POM–MHC-based composite materials.

It has been found that Anderson/Lindqvist/Wells–Dawson-type POMs can be covalently functionalized by tripodal alcohol ligands [e.g., tris(hydroxymethyl)aminomethane].<sup>6</sup> Inspired by the results, we propose a general step-by-step strategy to realize the combination of POMs with MHCs. First, the introduction of additional MHC-favorite functional groups into the tripodal alcohol ligands could be expected to form bitopic tripodal alcohol derivatives with the ability to serve as linkers between POMs and MHCs. Next, according to the literature,<sup>6</sup> the obtained bitopic tripodal alcohol derivatives could, in principle, be grafted onto the skeleton of different POMs to generate various L-functionalized POMs. Finally, targeted POM–MHC-based composite clusters could be achieved via assembly reactions of L-functionalized POMs with metal halide salts.

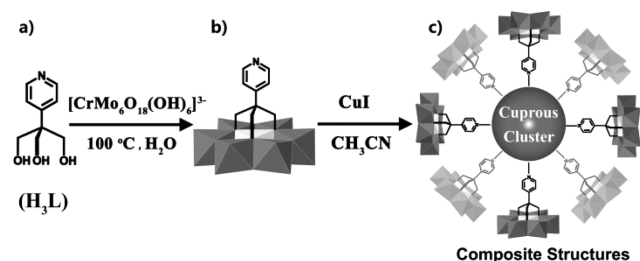
The above step-by-step strategy can be demonstrated in detail by the synthetic process of **1**, as shown in Scheme 1. To begin with, given that MHCs prefer nitrogen donors, a tripodal alcohol derivative L-containing pyridine group was synthesized according to the literature method and employed as a bitopic ligand in an attempt to cross-link POMs and MHCs.<sup>7</sup>

Next, an Anderson-type POM  $[\text{NH}_4]_3[\text{CrMo}_6\text{O}_{18}(\text{OH})_6]$  was prepared as a precursor according to the literature.<sup>8</sup> This is because (1) it is well-known that Anderson-type POMs  $\{\text{XMo}_6\text{O}_{18}(\text{OH})_6\}$  (X = Mn, Fe, Cr, etc.) are composed of six

Received: June 21, 2016

Published: August 11, 2016

### Scheme 1. Illustration of a Step-by-Step Strategy for Creating POM–MHC-Based Composite Structures



edge-sharing  $\text{MoO}_6$  octahedra, forming a planar hexagon around the central  $\text{XO}_6$  octahedron (Figure S1), where the six  $\mu_3$ -oxygen atoms surrounding the X center are hydroxyl groups that can be readily substituted by the  $-\text{OH}$  groups from tripodal alcohols and (2) the Anderson-type polyoxoanion  $[\text{CrMo}_6\text{O}_{18}(\text{OH})_6]^{3-}$  tends to form a mono-L-functionalized POM species in the presence of an equivalent amount of tripodal ligands under hydrothermal reactions,<sup>9</sup> which can act as a monodentate terminal ligand with a particular tendency for constructing isolated POM–MHC-based clusters.

Further, the assembly reaction of  $[\text{NH}_4]_3[\text{CrMo}_6\text{O}_{18}(\text{OH})_6]$  with L under hydrothermal conditions yields an expected asymmetric mono-L-functionalized POM,  $[\text{TBA}]_4[\text{CrMo}_6\text{O}_{18}(-\text{OH})_3\text{L}]\cdot\text{Br}\cdot\text{H}_2\text{O}$  (2; Scheme 1 and Figure 1a). The new polyoxoanion  $[\text{CrMo}_6\text{O}_{18}(\text{OH})_3\text{L}]^{3-}$  (2a) can be

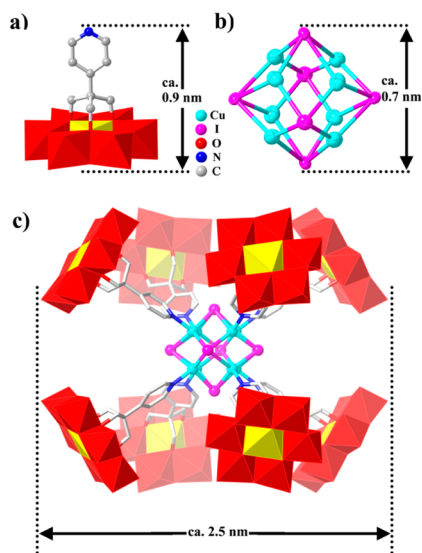


**Figure 1.** Structures of (a) 2a, (b)  $[\text{Cu}_8\text{I}_6]^{2+}$ , and (c) 1a, respectively. Color codes:  $\text{MoO}_6$ , red;  $\text{CrO}_6$ , yellow.

derived from the replacement of three  $\mu_3$ -OH groups of parent polyoxoanion  $[\text{CrMo}_6\text{O}_{18}(\text{OH})_6]^{3-}$  with three OH groups from the L ligand. One important structural feature of 2a is that the introduction of an uncoordinated pyridine group creates the possibility for encapsulating MHCs (Scheme 1c). Another structural feature is that 2a has another three  $\mu_3$ -OH groups located on the opposite face of the L ligand. These three  $\mu_3$ -OH groups are potential hydrogen-bonding acceptor groups for intriguing supramolecular assemblies.

Finally, the assembly of 2 with CuI successfully gives rise to an expected inorganic–organic hybrid POM–MHC-based cluster 1 with some remarkable structural features. The first is that 1

crystallizes in the tetragonal space group  $I4/m$  and its molecular structure consists of two kinds of completely different metal clusters with different charge properties: the cationic high-nuclearity cuprous iodide cluster  $[\text{Cu}_8\text{I}_6]^{2+}$  with a size of ca.  $0.7 \times 0.7 \times 0.7$  nm and the anionic L-functionalized polyoxomolybdate  $[\text{HCrMo}_6\text{O}_{18}(\text{OH})_3\text{L}]^{2-}$  with a size of ca.  $0.9 \times 0.8 \times 0.8$  nm. The  $[\text{Cu}_8\text{I}_6]^{2+}$  cluster was first reported in 2012,<sup>10</sup> whose configuration can be viewed as a highly symmetrical octahedron with its eight centroids and six vertexes occupied by eight  $\text{Cu}^+$  ions and six  $\mu_4\text{-I}^-$  ions (Figure 1b), respectively.

The second is that, through coordination bonds between  $\text{Cu}^+$  ions and pyridyl nitrogen atoms, every  $[\text{Cu}_8\text{I}_6]^{2+}$  cluster is linked to eight POMs  $[\text{HCrMo}_6\text{O}_{18}(\text{OH})_3\text{L}]^{2-}$ , resulting in the first POM–MHC-based composite cluster  $\{[\text{Cu}_8\text{I}_6]-[\text{HCrMo}_6\text{O}_{18}(\text{OH})_3\text{L}]_8\}^{14-}$  (1a; Figure 1c). Alternatively, the large cluster 1a can be described as a nanosized (ca. 2.5 nm) cubelike molecule with its body-centered-cubic site and eight vertexes respectively occupied by one  $[\text{Cu}_8\text{I}_6]^{2+}$  cluster and eight Anderson-type POMs  $[\text{HCrMo}_6\text{O}_{18}(\text{OH})_6]^{2-}$  held together by eight L ligands.

The third is that the nanosized clusters 1a can elaborately self-assemble into a uniform and porous 3D supramolecular framework with 1D tetragonal channels along the *a*-axis direction (Figure S2). In 1, there are strong  $\text{O}\cdots\text{H}-\text{O}$  [2.589(8)–2.596(9) Å] intermolecular hydrogen bonds between terminal oxygen atoms and  $\mu_3$ -OH groups of adjacent 1a polyoxoanions (Table S1 and Figure S3). With hydrogen bonds, every 1a is joined to eight adjacent ones to form the 3D supramolecular network with 8-connected *bcu* topology. Intriguingly, a side view of the 1D channels in 1 indicates that they can be viewed as edge-sharing supramolecular octahedral cages (Figure S3), in which every huge supramolecular octahedral cage (ca.  $5.0 \times 5.0 \times 3.9$  nm in dimensions) is formed by 6  $[\text{Cu}_8\text{I}_6]^{2+}$  clusters and 16  $[\text{HCrMo}_6\text{O}_{18}(\text{OH})_3\text{L}]^{2-}$  polyoxomolybdates located at the vertex sites and middle sites of the edges (Figures S4,S), respectively. PLATON calculation indicates that the extra-framework volumes per unit cell for 1 is  $22521.5 \text{ \AA}^3$  (70.3% of the total unit cell volume).<sup>11</sup> The bulky TAB cations are dispersed in cavities, playing the role of charge compensation and framework stabilization. However, only 4/7 of TAB cations can be clearly mapped in the single-crystal structure analysis because of the highly porous and symmetric characteristics of the supramolecular network.

Different from the isolated molecular cluster 1, quite recently, we also made the first two high-dimensional (2D and 3D) POM–MHC-based cluster–organic frameworks  $(\text{TAB})_6[\text{Cu}_2\text{I}_2][\text{MnMo}_6\text{O}_{18}(\text{L})_2]_2$  and  $(\text{TAB})_6[\text{Cu}_4\text{I}_4][\text{MnMo}_6\text{O}_{18}\text{L}_2]_2$ .<sup>12</sup> The key point to control the formation of isolated composite clusters or extended composite frameworks lies in the use of different Anderson-type POM precursors. As mentioned above, reacting with an equivalent amount of tripodal ligands, polyoxoanion  $[\text{CrMo}_6\text{O}_{18}(\text{OH})_6]^{3-}$  forms mono-L-functionalized 2a, which will act as a terminal ligand for the construction of molecular clusters. Unlike  $[\text{CrMo}_6\text{O}_{18}(\text{OH})_6]^{3-}$ , polyoxoanions such as  $[\text{MnMo}_6\text{O}_{18}(\text{OH})_6]^{3-}$  and  $[\text{FeMo}_6\text{O}_{18}(\text{OH})_6]^{3-}$  prefer to form bi-L-functionalized species even in the presence of an equivalent amount of tripodal ligands.<sup>13</sup> And thus, during the course of self-assembly reactions, these bi-L-functionalized POMs will act as bridging ligands to cross-link MHCs to form extended structures. Additionally, it is worth noting that the copper nuclearity of incorporated copper halide cores has been increased from binuclear  $\{\text{Cu}_2\text{I}_2\}$  and tetranuclear  $\{\text{Cu}_4\text{I}_4\}$  cores in the extended structures

(TAB)<sub>6</sub>[Cu<sub>2</sub>I<sub>2</sub>][MnMo<sub>6</sub>O<sub>18</sub>(L)<sub>2</sub>]<sub>2</sub> and (TAB)<sub>6</sub>[Cu<sub>4</sub>I<sub>4</sub>]-[MnMo<sub>6</sub>O<sub>18</sub>L<sub>2</sub>]<sub>2</sub> to an octanuclear {Cu<sub>8</sub>I<sub>6</sub>} core in the cluster **1**.

The phase purity of **1** was confirmed by the powder X-ray diffraction (PXRD) patterns in comparison with the simulated single-crystal data of **1** (Figure S6). The variable-temperature magnetic susceptibility of **1** was measured in the temperature range of 2–300 K with an applied magnetic field of 1 kOe. The temperature dependence of  $\chi_m$  and  $\chi_m T$  is shown in Figure S7. The value of  $\chi_m$  slowly increases from 0.05 cm<sup>3</sup> mol<sup>-1</sup> K at 300 K to 0.25 cm<sup>3</sup> mol<sup>-1</sup> K at 40 K and then exponentially to the maximum of 5.45 cm<sup>3</sup> mol<sup>-1</sup> K at 2 K. At 300 K, the experimental  $\chi_m T$  value of **1** is 15.29 cm<sup>3</sup> mol<sup>-1</sup> K per formula unit, being consistent with the theoretical value (15.00 cm<sup>3</sup> mol<sup>-1</sup> K) expected for eight uncoupled high-spin Cr<sup>3+</sup> ions with  $S = 3/2$  and  $g = 2.0$ . Upon cooling, the  $\chi_m T$  value slowly decreases to 12.11 cm<sup>3</sup> mol<sup>-1</sup> K at 15 K and then rapidly reaches the minimum of 9.79 cm<sup>3</sup> mol<sup>-1</sup> at 2 K. Such magnetic behaviors suggest the ferromagnetic property of **1**, which is a typical character for compounds containing high-spin Cr<sup>III</sup> ions.<sup>14</sup> The temperature dependence of the reciprocal susceptibility ( $1/\chi_m$ ) obeys the Curie–Weiss law above 75 K with a negative Weiss constant  $\theta = -24.56$  K and Curie constant  $C = 16.52$  cm<sup>3</sup> mol<sup>-1</sup> (Figure S8), which confirm the antiferromagnetic property of **1**. The UV/vis diffuse-reflectance spectra (Figure S9) of the polycrystalline sample showed that the band gap of **1** can be calculated as 1.75 eV, indicating that **1** is a potential semiconductor.

In summary, the first inorganic–organic hybrid POM–MHC-based molecular cluster **1** has been created, which demonstrates a feasible step-by-step synthetic method for making inorganic–organic hybrid composite clusters. Considering that there are various POMs, MHCs, and tripodal alcohol derivatives, the method reported here is general and shows the great potential for creating a large family of novel POM–MHC-based composite functional materials.

## ■ ASSOCIATED CONTENT

### ■ Supporting Information

The Supporting Information is available free of charge on the ACS Publications website at DOI: 10.1021/acs.inorgchem.6b01453.

Experimental details, crystallographic data for **1** and **2**, additional structural figures and additional characterizations (PDF)

X-ray crystallographic data in CIF format (CIF)

X-ray crystallographic data in CIF format (CIF)

## ■ AUTHOR INFORMATION

### Corresponding Authors

\*E-mail: stzheng@fzu.edu.cn.

\*E-mail: ygy@bit.edu.cn.

### Notes

The authors declare no competing financial interest.

## ■ ACKNOWLEDGMENTS

This work was financially supported by the National Natural Science Foundations of China (Grants 21303018, 21371033, and 21401195), the Natural Science Foundation for Young Scholars of Fujian Province (Grant 2015J05041), and Projects from State Key Laboratory of Structural Chemistry of China (Grants 20150001 and 20160020).

## ■ REFERENCES

- (a) Ma, F. J.; Liu, S. X.; Sun, C. Y.; Liang, D. D.; Ren, G. J.; Wei, F.; Chen, Y. G.; Su, Z. M. *J. Am. Chem. Soc.* **2011**, *133*, 4178–4181.
- (b) Nohra, B.; El Moll, H.; Rodriguez Albelo, L. M.; Mialane, P.; Marrot, J.; Mellot-Draznieks, C.; O’Keeffe, M.; Ngo Biboum, R.; Lemaire, J.; Keita, B.; Nadjo, L.; Dolbecq, A. *J. Am. Chem. Soc.* **2011**, *133*, 13363–13374.
- (c) Qin, J. S.; Du, D.-Y.; Guan, W.; Bo, X. J.; Li, Y. F.; Guo, L.-P.; Su, Z. M.; Wang, Y.-Y.; Lan, Y. Q.; Zhou, H. C. *J. Am. Chem. Soc.* **2015**, *137*, 7169–7177.
- (2) (a) Lykourinou, V.; Chen, Y.; Wang, X. S.; Meng, L.; Hoang, T.; Ming, L. J.; Musselman, R. L.; Ma, S. *J. Am. Chem. Soc.* **2011**, *133*, 10382.
- (b) Li, Z.; Zeng, H. C. *Chem. Mater.* **2013**, *25*, 1761–1768.
- (c) Liu, Y.; Zhang, W.; Li, S.; Cui, C.; Wu, J.; Chen, H.; Huo, F. *Chem. Mater.* **2014**, *26*, 1119–1125.
- (d) Gao, J. K.; Miao, J.; Li, Y. X.; Ganguly, R.; Zhao, Y.; Lev, O.; Liu, B.; Zhang, Q. C. *Dalton Trans.* **2015**, *44*, 14354–14358.
- (e) Gao, J. K.; Cao, S. W.; Tay, Q. L.; Liu, Y.; Yu, L. M.; Ye, K. Q.; Mun, P. C. S.; Li, Y. X.; Rakesh, G.; Loo, S. C. J.; Chen, Z.; Zhao, Y.; Xue, C.; Zhang, Q. C. *Sci. Rep.* **2013**, *3*, 1853–1857.
- (3) (a) Oms, O.; Dolbecq, A.; Mialane, P. *Chem. Soc. Rev.* **2012**, *41*, 7497–7536.
- (b) Zang, H. Y.; Miras, H. N.; Long, D. L.; Rausch, B.; Cronin, L. *Angew. Chem., Int. Ed.* **2013**, *52*, 6903–6906.
- (c) Du, D. Y.; Qin, J. S.; Li, S. L.; Su, Z. M.; Lan, Y. Q. *Chem. Soc. Rev.* **2014**, *43*, 4615–4632.
- (d) Ma, P. T.; Wan, R.; Wang, Y. Y.; Hu, F.; Zhang, D. D.; Niu, J. Y.; Wang, J. P. *Inorg. Chem.* **2016**, *55*, 918–924.
- (e) Liu, Z. J.; Wang, X. L.; Qin, C.; Zhang, Z. M.; Li, Y. G.; Chen, W. L.; Wang, E. B. *Coord. Chem. Rev.* **2016**, *313*, 94–110.
- (f) Surman, A. J.; Robbins, P. J.; Ujma, J.; Zheng, Q.; Barran, P. E.; Cronin, L. *J. Am. Chem. Soc.* **2016**, *138*, 3824–3830.
- (4) (a) Kang, Y.; Wang, F.; Zhang, J.; Bu, X. H. *J. Am. Chem. Soc.* **2012**, *134*, 17881.
- (b) Deshmukh, M. S.; Yadav, A.; Pant, R.; Boomishankar, R. *Inorg. Chem.* **2015**, *54*, 1337–1345.
- (5) (a) Mohapatra, B.; Verma, S. *Cryst. Growth Des.* **2016**, *16*, 696–704.
- (b) Wang, G. E.; Xu, G.; Liu, B. W.; Wang, M. S.; Yao, M. S.; Guo, G. C. *Angew. Chem., Int. Ed.* **2016**, *55*, 514–518.
- (6) (a) Song, Y. F.; McMillan, N.; Long, D. L.; Thiel, J.; Ding, Y. L.; Chen, H.; Gadegaard, N.; Cronin, L. *Chem. - Eur. J.* **2008**, *14*, 2349–2354.
- (b) Pradeep, C. P.; Misdrahi, M. F.; Li, F. Y.; Zhang, J.; Xu, L.; Long, D. L.; Liu, T. B.; Cronin, L. *Angew. Chem., Int. Ed.* **2009**, *48*, 8309–8313.
- (c) Saad, A.; Zhu, W.; Rousseau, G.; Mialane, P.; Marrot, J.; Haouas, M.; Taulelle, F.; Dessapt, R.; Serier-Brault, H.; Riviere, E.; Kubo, T.; Oldfield, E.; Dolbecq, A. *Chem. - Eur. J.* **2015**, *21*, 10537–10547.
- (d) Zhang, J.; Liu, Z.; Huang, Y.; Zhang, J.; Hao, J.; Wei, Y. *Chem. Commun.* **2015**, *51*, 9097–9100.
- (7) Menozzi, D.; Biavardi, E.; Massera, C.; Schmidtchen, F.; Cornia, A.; Dalcanele, E. *Supramol. Chem.* **2010**, *22*, 768–775.
- (8) Nomiya, K.; Takahashi, T.; Shirai, T.; Miwa, M. *Polyhedron* **1987**, *6*, 213–218.
- (9) (a) Lin, C. G.; Chen, W.; Long, D. L.; Cronin, L.; Song, Y. F. *Dalton Trans.* **2014**, *43*, 8587–8590.
- (b) Wu, P. F.; Yin, P. C.; Zhang, J.; Hao, J.; Xiao, Z. C.; Wei, Y. G. *Chem. - Eur. J.* **2011**, *17*, 12002–12005.
- (10) Xin, B. J.; Zeng, G.; Gao, L.; Li, Y.; Xing, S. H.; Hua, J.; Li, G. H.; Shi, Z.; Feng, S. H. *Dalton Trans* **2013**, *42*, 7562–7568.
- (11) Spek, A. L. *PLATON*; Utrecht University: Utrecht, The Netherlands, 2003.
- (12) Li, X. X.; Wang, Y. X.; Wang, R. H.; Cui, C. Y.; Tian, C. B.; Yang, G. Y. *Angew. Chem., Int. Ed.* **2016**, *55*, 6462–6576.
- (13) Zhang, J.; Hao, J.; Wei, Y. G.; Xiao, F. P.; Yin, P. C.; Wang, L. S. *J. Am. Chem. Soc.* **2010**, *132*, 14–15.
- (14) Fernández-Armas, S.; Mesa, J. L.; Pizarro, J. L.; Clemente-Juan, J. M.; Coronado, E.; Arriortua, M. I.; Rojo, T. *Inorg. Chem.* **2006**, *45*, 3240–3248.